13B.2 **ANALYSIS OF CROSS-SPECTRUM SUPERCELLS DURING THE NORTH GEORGIA TORNADO EVENT OF 2 JANUARY 2006**

Trisha D. Palmer*, Lans P. Rothfusz, Steven E. Nelson
NOAA/National Weather Service Forecast Office Atlanta, Peachtree City, Georgia

Brandon A. Miller
Georgia Institute of Technology, Atlanta, Georgia

1. INTRODUCTION

Classifying supercells based on the amount and spatial distribution of precipitation has been a common practice in both the research and operational fields of meteorology for many years (Doswell et al. 1990, hereafter referred to as D90; Doswell and Burgess 1993, hereafter referred to as D&B93). The common supercell classifications are low-precipitation (LP), classic (CL), and high-precipitation (HP) (D90), although operationally observed supercells range across the supercell spectrum. The most common type of supercell observed is the HP (Johns et al. 1993), especially east of the Mississippi river (D&B93). A vast majority of the rest of the supercells found in the eastern United States fall under the classic type, especially those associated with strong tornadoes (D&B93). LP supercells are often associated with the western portions of the Great Plains due to the frequent presence of a surface dryline, which is virtually a necessity for the environment of these storms (Bluestein and Parks 1983; Moller et al. 1994). Since drylines rarely propagate east of the Mississippi River, LP supercells are extremely rare occurrences in the southeastern United States. LP supercells are rarely tornadic, and usually only become so if their structure evolves to become more classic in nature (D&B93).

On the afternoon of 2 January 2006, several storms formed in Georgia which spanned the spectrum of supercell classifications (Fig. 1). Though the storms of interest formed in a small spatial area (approximately 50 km apart), they displayed vastly different characteristics throughout their life cycles. The unique character of the storms can be attributed to the variety of mesoscale influences in the near-storm environment. The storms formed along a dryline that propagated eastward across Alabama during the day. Meanwhile, much of northeastern

* *Corresponding author address*: Trisha D. Palmer, National Weather Service, 4 Falcon Drive, Peachtree City, GA, 30269; e-mail: trisha.palmer@noaa.gov

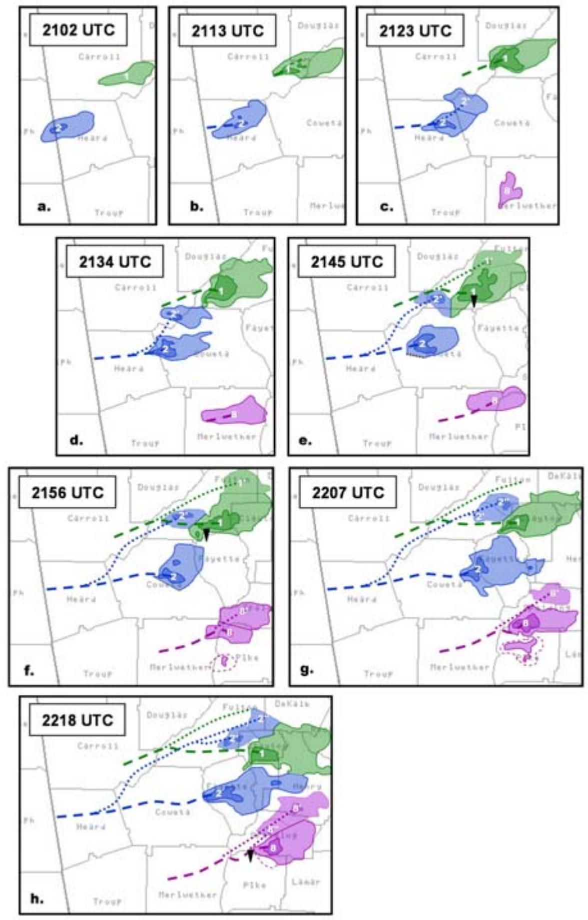

Fig. 1. Schematic of splitting and merging storms and their paths. Contours are 30 and 50 dBZ reflectivities. Dashed contours near S8 (Fig. f., g., and h.) indicate 20 dBZ shower. Black dotted lines on south edge of S2 indicate adjacent storm reflectivities omitted for figure clarity. Bottom point of inverted black triangles (S1 and S8) show approximate tornado locations. Primes (´) indicate storm splits. Labeled storms are numbered non-sequentially to account for additional supercells that occurred during the outbreak but were not included in the figure for clarity.

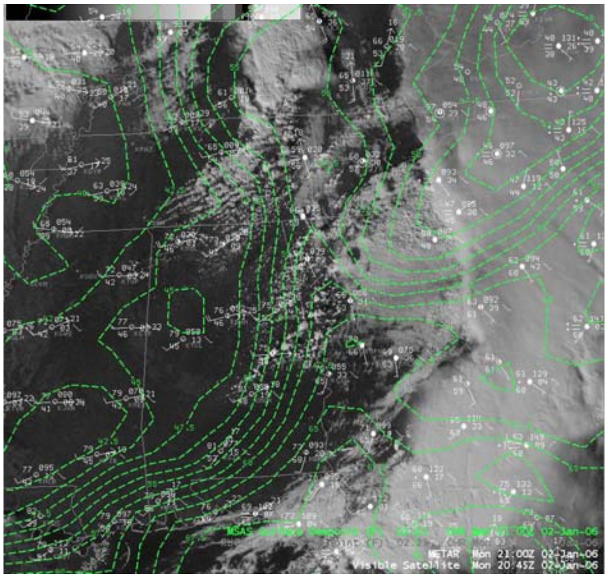

Fig. 2. Surface conditions near the time of convective initiation. Note, from the satellite image, the cold front from central Tennessee into northwest Mississippi, the dryline in eastern Alabama, and the CAD in northeast Georgia.

Georgia was in an area of cold-air damming (CAD) (Bell and Bosart 1988), with a majority of the severe weather taking place just south of the intersection of these two boundaries (Fig. 2). The purpose of this paper is twofold: To describe the cross-spectrum nature of two of the supercells from 2 January 2006, Supercell 1 (S1) and Supercell 8 (S8); and to discuss the observation that each of the six tornadoes from this event was the result of a storm merger.

Supercell S1 (Fig. 1) was the northernmost supercell to form along the dryline, and the closest to the cold-air damming "wedge" front. It produced hail 2 in (over 5 cm) in diameter, as well as an F2 tornado on the legacy Fujita scale leaving a path just over 11 km long and 1.5 km wide in the communities of Palmetto (Fulton County) and Tyrone (Fayette County). The storm followed a lifecycle similar to an archetypal Great Plains classic supercell (D90).

Supercell S8 (Fig. 1) formed approximately 48 km south of S1 and was slightly ahead of the main line of storms. It produced the strongest tornado of the day – an F3 which moved a house over 18 m from its foundation and tossed two vehicles almost 230 m near the community of Hollonville (northwest Pike County). The path of this significant tornado was 4.8 km long and 1.5 km wide. As will be shown later in the paper, S8 displayed LP characteristics during the first part of its lifecycle, later becoming classic and eventually HP in nature (D90; D&B93).

Palmer et al. (2008, manuscript submitted to the *Digest*) will contain a comprehensive overview of the synoptic, mesoscale, and storm-scale environments, while this manuscript provides only a brief overview of some of these elements.

2. MESOSCALE ENVIRONMENT

2.1. *Dryline*

The dryline, recognized as a north-south oriented horizontal moisture gradient traditionally located in the central and southern plains of the United States, is often evaluated by severe thunderstorm forecasters as a prime area for convective development (Rhea 1966). The dryline is normally confined to the western plains, but in rare events, the dryline can be intensified and carried eastward during large-scale translating weather events such as low pressure centers (Hane et al. 1993; Hane et al. 2001). This eastward translation of the dryline was the case during the 2 January 2006 tornado event. As the parent upper-level low tracked from eastern Colorado across the Missouri River Valley and into the Ohio River Valley from 1200 UTC on 1 January to 0000 UTC on 3 January, the dryline remained approximately 250 km southeast of the surface cold front, the latter of which was in central Tennessee around the time of CI. The dryline and cold front can be seen both in surface analyses and also visible boundaries in satellite images (Fig. 2). At 1600 UTC the ASOS near Birmingham, Alabama (KBHM), had a 17^{o}C (62^{o}F) dewpoint with a 22^{o}C (71^{o}F) surface temperature and winds from 240 degrees. At 2000 UTC, after the passage of the dryline, the same station reported a 9^{o}C (48^{o}F) dewpoint with a surface temperature of 25^{o}C (77^{o}F) and winds from 250 degrees. Meanwhile, the surface cold front remained approximately 160 km northwest of KBHM at 2000 UTC, marked by a 12^{o}C (10^{o}F) temperature decrease and 70 degree wind shift. The presence of this dryline, as well as its relative increase in intensity, helped to increase moisture convergence and provide sufficient upward vertical motion needed to initiate convection on 2 January.

2.2. *Cold-air damming*

Appalachian cold-air damming (CAD) refers to the phenomenon of cold air becoming entrenched along the eastern slopes of Appalachian Mountains through a process of geostrophic adjustment (Richwien 1980, Bell and Bosart 1988). The geostrophic adjustment results in a dome of cool, stable air and is most easily identified by a "U"-shape in the isobars on a sea level pressure map, but can also be seen in a θ_e trough ("U"-shaped as well) against the lee of the mountains. The front that develops between the CAD and the surrounding airmass resembles quasi-stationary warm fronts that can maintain temperature contrasts of more than 10^{o}C in less than 100 km (Bosart 1975). This front, often termed the "wedge" front or Piedmont front due to its common location over the Piedmont, can also become a focal point for potentially severe convection (Businger et al. 1991; Vescio et al. 1993).

The CAD scenario in place during the 2 January 2006 event was that of a "hybrid" CAD, in which the central mean sea level pressure of the parent high is less than 1030 hPa and diabatic processes contribute to the CAD onset (Bailey et al. 2003). One of the most difficult challenges facing a forecaster in this region is the prediction of cold dome demise (Keeter et al. 1995). CAD erosion takes place when the inversion separating the topographically trapped air from the free atmosphere is mixed out via any of several processes, such as thermal advection, solar heating, a frontal passage, etc. (Lackmann and Stanton 2004). The erosion mechanism influential in the demise of the hybrid CAD in place on 2 January was a "cold frontal passage". During this erosion mechanism, the cold front is influential in the demise of the CAD event, whereas in other erosion scenarios (e.g., "northwestern low"), the CAD has eroded before the front arrives (Stanton 2003).

During the early morning of 2 January, any erosion of the CAD prior to the cold front's arrival could have significantly influenced the mesoscale environment by weakening the low-level convergence, moisture pooling, and baroclinicity in the area of the wedge front. The eroding was not observed, however, likely due to the morning convection and associated mid- and high-level clouds above a thick low-level stratus layer in the CAD region. This cloud cover (seen in Fig. 2) inhibited the aforementioned diabatic heating to begin eroding the CAD. While it was believed at the time of the event that the morning convection could stabilize the environment via reduced solar insolation and thus decrease the chance for severe weather later in the day, it may have actually played an important role in its eventual occurrence by strengthening the CAD via the very mechanism of reduced insolation over the CAD region. Conversely, cloud cover south of the CAD broke up into cumulus streets in the high θ_e air, allowing the temperatures to warm further (to between 20-25^{o}C [68-77^{o}F]), which increased the baroclinicity along and to the south and west of the wedge front.

2.3. *Other mesoscale parameters*

The morning convection nearly cleared Alabama completely by 1600 UTC (local noon), and provided ample solar heating time for surface temperatures to rise to 27^{o}C (80^{o}F) in southern Alabama. In the moisture-rich area ahead of the dryline, mesoanalyses produced by the Storm Prediction Center showed surface-based CAPE values increased to between 1000 and 2000 J kg^{-1} in eastern Alabama between 1500 and 2000 UTC. 100 hPa mixed-layer CAPE (MLCAPE) values were well over 1000 J kg^{-1} in these same areas, consistent with (and perhaps slightly higher than) the findings of Guyer et al. (2006, hereafter referred to as G06). Analysis of the 1800 UTC sounding data from KBMX showed a surface-based CAPE (SBCAPE) value of 1991 J kg^{-1}, while the KFFC sounding showed SBCAPE of 565 J kg^{-1}, increasing to 1633 J kg^{-1} at 0000 UTC. The sounding data illustrate how the instability was increasing and spreading eastward in the clear air behind the morning convection. Based on these data, a moderately unstable environment with SBCAPEs approaching 2000 J kg^{-1} can be inferred in the location of CI of the storms.

According to Craven et al. (2002), low-level

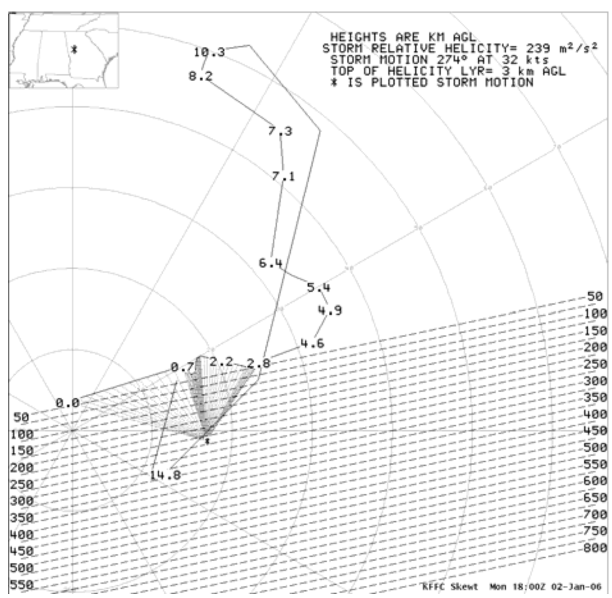

Fig. 3. Hodograph derived from the 1800 UTC upper-air rawindsonde observation from KFFC.

shear (0-1 km) values greater than 8-10 m s^{-1} (15-20 kt) have been associated with significant tornado development in supercells. On the afternoon of 2 January 2006, 0-1 km shear values of approximately 15-21 m s^{-1} (30-40 kt) were located throughout the region of the storm development. These values are in the upper two quartiles associated with F2 and greater tornadoes in Gulf Coast storms, according to G06. Deep layer shear (0-6 km) is another important factor specifically in storm development and sustenance, with values of 18-21 m s^{-1} (35-40 kt) and greater associated with supercells (Rasmussen and Blanchard 1998). For 2 January, deep-layer shear values of approximately 30 m s^{-1} (60 kt) were located in the area of CI. The storms moved into areas of even higher (>35 m s^{-1} [>70 kt]) deep-layer shear after 2300 UTC. From the study done by G06, the large area of 0-6 km shear of greater than 30 m s^{-1} (60 kt) is in the upper quartile of their climatological database; the area of 35 m s^{-1} (70 kt) is beyond the 90th percentile of the G06 database. Storm relative helicity (SRH) values between the surface and 1 km (e.g., Davies-Jones et al. 1990) ranged from 300 to 500 m^2 s^{-2} through the afternoon hours on 2 January, mostly in excess of the upper quartile of storms studied by G06. Similarly, 0-3 km SRH also mainly ranged from 300 to 500 m^2 s^{-2}, but surpassed 600 m^2 s^{-2} in parts of northeast Georgia, in the southern reaches of the CAD, which is common in these areas. These SRH values were mainly in the upper one to two quartiles of storms studied by G06. The hodograph provided by the 1800 UTC KFFC sounding (Fig. 3) indicated 239 m^2 s^{-2} of 0-3 km SRH; this was before CI. The significant amount of shear throughout the environment most certainly helped the storms not only to initiate, but also helped the storms to maintain their intensity, even after leaving areas of higher instability.

3. STORM-SCALE ANALYSIS

Characteristics of S1 versus S8 as seen from the WSR-88D (KFFC) in Peachtree City were vastly different. While these storms must be evaluated individually before direct comparisons can be made, one storm-scale feature that was applicable to all storms that day was the storm motion and behavior: the lowest 4-6 km represented by the straight-line hodograph in Fig. 3 supports splitting storms. This is an important feature that factored into the 2 January event.

3.1. *Supercell S1*

S1 showed all the signs of a classic supercell (D90, D&B93), especially as it evolved into its tornadic phase. For example, the presence of a deep, persistent mesocyclone was noted within 30 minutes of the storm's initiation at approximately 2045 UTC. Deviant rightward motion and a hook echo developed as the storm evolved as well.

S1 did not show any signs of low-level rotation until 2113 UTC. By 2134 UTC, the first hook echo emerged at the 0.5^{o} slice, in extreme southwest Fulton County. By 2140 UTC, the reflectivities aloft in S2′ to the southwest of S1 began to graze the back edge of the hook echo, and rotational velocities increased slightly at the 3.1^{o} elevation scan. At 2145 UTC, 35-40 dBZ echoes from S2′ can be seen to intersect the hook echo of S1, and low-level rotation increased significantly, with rotational velocity increasing by over 7 m s^{-1} (almost 14 kt), from 16.2 m s^{-1} to 23.3 m s^{-1} (31.5 kt to 45.3 kt) (with a 1 nm mesocyclone diameter) between this and the previous 0.5^{o} scan. The first tornado of the day touched down at this time, remaining on the ground from 2145-2156 UTC. As the storm was producing F2 damage in the community of Tyrone in northern Fayette County (Fig. 4), the left-mover that grazed the hook echo can clearly be seen, still traveling to the north-northeast, to the northwest of the tornadic supercell (i.e., a non-merger interaction, after Lee et al. 2006). By 2207 UTC, the tornado had lifted and only an appendage remained of the hook echo, but the storm transitioned to HP (not shown) and remained severe for another 20 minutes, producing hail up to 1.75 in (4.4 cm). The storm would interact with other storms (see below), but it eventually dissipated in more stable air just south of the wedge front. While not actually within the cold dome, this area remained relatively stable due to persistent stratus clouds through the afternoon hours and had not destabilized as it did to the south and southwest.

As mentioned above, tornadogenesis occurred as S2′ grazed the hook echo of S1. It is possible that precipitation loading from anvil hydrometeors or evaporative cooling underneath the anvil of S2′ contributed to the descent needed to allow the RFD to form, thereby allowing for near-simultaneous tightening and lowering of the mesocyclone (Markowski 2002). However, Markowski et al. (2002) seem to indicate that evaporational cooling and/or entrainment of mid-level cool air is not as important as previously thought, in regards to tornadic supercells. Without sufficient observations or model simulations of the

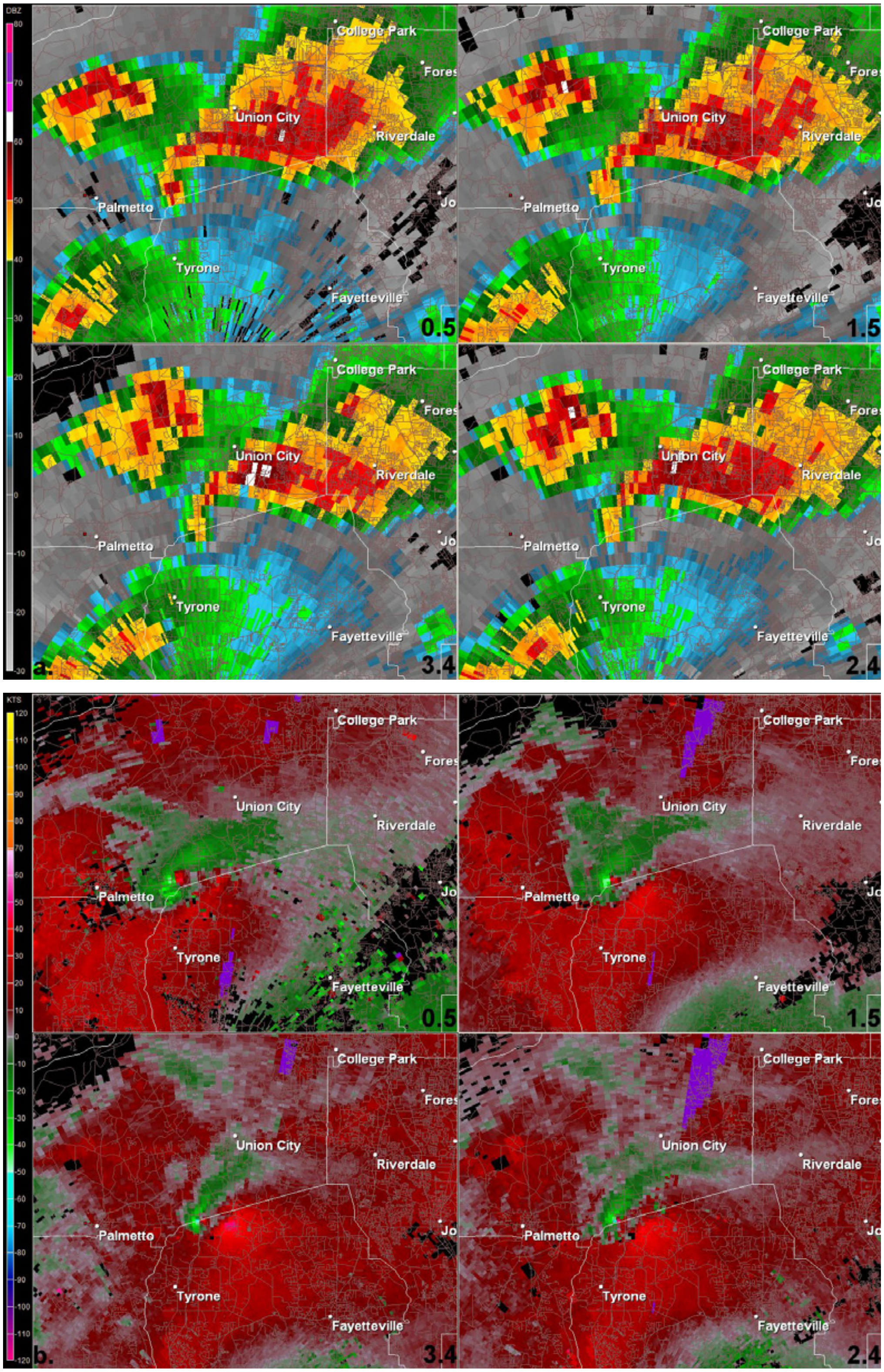

Fig. 4. GR2Analyst (a) reflectivity and (b) storm-relative velocity image from KFFC of S1 at 2156 UTC as it produced F2 damage near the community of Tyrone in northern Fayette County. Clockwise from upper left in both images: 0.5°, 1.5°, 2.4°, and 3.4°.

storm, it is impossible to know if this was the case fact that tornadogenesis occurred just as S2' contacted S1, however, does raise the question as to whether or not tornadogenesis would have occurred without this series of events.

3.2. *Supercell S8*

Although S8 produced the strongest tornado of the day (an F3 resulting in three injuries), its structure and evolution were significantly different from the classic S1. Using the same thresholds as with S1, the first discernible echo associated with S8 appeared at 2102 UTC. The storm developed approximately 25 km southeast of the main line of convection and was characterized by much lower reflectivity values through initial tornadogenesis. This is in agreement with the finding of Bluestein and Parks (1983) that LP storms form as isolated cells, "often to the south of a broken line of existing storms;" and were supercells in this case.

By 2207 UTC, weak rotation had been detected, but was not collocated with S8; that is, the rotation appeared detached from the storm itself. No other well-defined rotation was evident with this storm prior to tornadogenesis. The short-lived F3 tornado touched down at 2212 UTC and traveled east across Pike County roughly during two volume scans (Fig. 5), lifting at 2218 UTC. No hook echo or appendage from the main cell was evident, even in reflectivity data aloft. The small area of 50 dBZ at 0.9^{o} at 2218 UTC in Fig. 5 (notated) is likely tornado debris, acting as scatterers. Very weak reflectivity values, on the order of 10-15 dBZ are all that exist as a connection between the area of tornado debris and the FFD in lower elevation scans (in fact, the first true hook echo emerged from S8 at 0.5^{o} between 2235-2240 UTC). Using the cross-section analysis of reflectivity at 2218 UTC, however, a narrow axis of 30 to 50 dBZ returns is apparent extending upward from the low level reflectivity associated with the tornado debris to the elevated higher reflectivity with the FFD (Fig. 6). Note the 9 km area of little or no reflectivity from the surface to 1500 m AGL from near the location of the tornado debris to the FFD.

At approximately 2130 UTC, a shower to the southwest of S8 developed and began moving northeast, into the inflow of S8. The shower was fully ingested in S8's weak echo region (WER) at the radar scan beginning at 2212 UTC – just as tornadogenesis was believed to occur (Fig. 1). As with S1, it is possible that precipitation loading from this merger provided the downdraft necessary to tilt horizontal vorticity and produce large vertical vorticity values at the surface in order to lead to tornadogenesis (Markowski 2002).

With both S8 and S1, the conclusions found by Lee et al. (2006) are applicable. Although their analysis involved only a single outbreak, they found that tornadoes were associated with 57% of mergers that involved supercells. They concluded that special attention should be paid to storm mergers; they could be an indicator of "heightened tornado threat, especially when the background storm environment features high relative humidity and low LCLs…" For the 2 January event, 100 hPa mixed level LCLs (MLLCLs) were at or below 600 m AGL until dryline passage. In the Craven et al. (2002) study, they found that the median value of MLLCL for significant tornadoes was between 750 and 1000 m, thus the 2 January case was most certainly characterized by low LCLs, and surface data indicated high relative humidity. Lee et al. (2006) also recommended the identification of "developing weaker cells whose anticipated paths could intersect the projected position of a preexisting supercell…" as "there exists at least circumstantial evidence that subsequent cell mergers with a supercell may prompt cyclic tornadogenesis." This describes the situation with S8 very well; as it eventually evolved into more of an HP supercell, going on to produce three more tornadoes (two F1s and an F0) after the tornado near Hollonville.

The observations from 2 January, and S8 in particular, also support the hypothesis set forth in Wurman et al. (2007). They suggest that a storm merger can enhance or trigger tornadogenesis by increasing the stretching of low-level vertical vorticity. In addition, by introducing rain-cooled air into the updraft, the merger can then subsequently disrupt that same stretching mechanism, thereby hastening the dissipation process, possibly resulting in short-lived tornadoes.

4. CONCLUSIONS

The unique near-storm environment in North Georgia on 2 January 2006, consisting of an unusually high θ_e January airmass, cold-air damming beginning to erode, an approaching dryline, splitting storms and storm mergers, combined with strong synoptic forcing allowed for an atypical wintertime outbreak in which supercells crossed the spectrum of classifications. In comparing the lifecycles of S1 and S8 as they produced the two most significant tornadoes of the day, the differences between the two are profound.

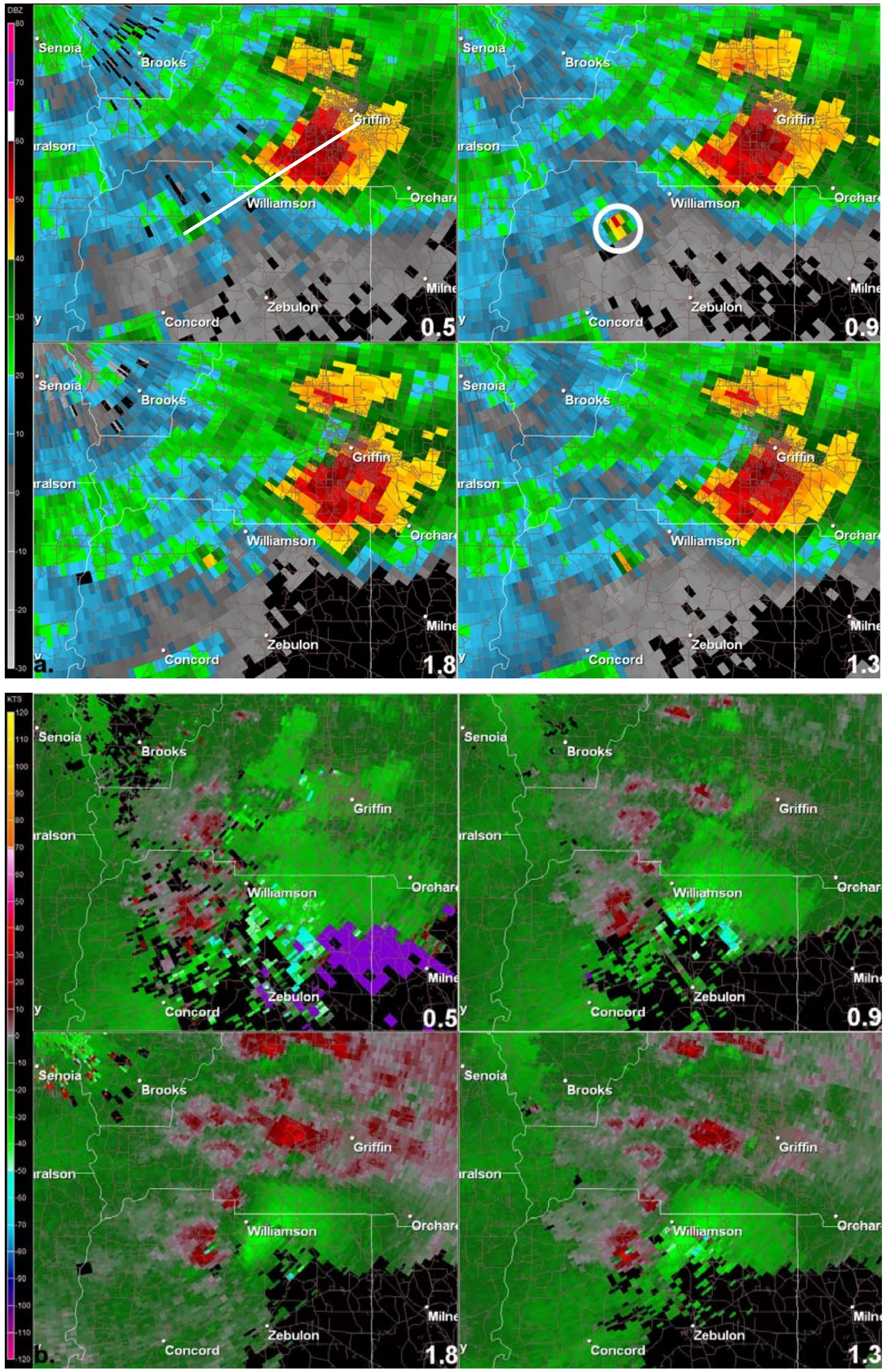

Fig. 5. GR2Analyst (a) reflectivity and (b) storm-relative velocity image image from KFFC of storm S8 at 2218 UTC as it produced F3 damage near the community of Hollonville in northwest Pike County. Clockwise from upper left in both images: 0.5°, 0.9°, 1.3°, and 1.8°. White line indicates cross-section location for Fig. 6.

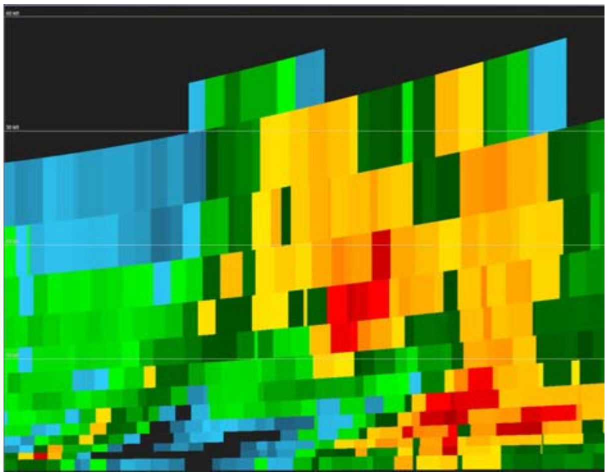

Fig. 6. GR2Analyst reflectivity cross-section from KFFC of S8 at 2218 UTC as the tornado touched down near the community of Hollonville in northwest Pike County.

Supercell S1, which developed along the dryline, developed as a classic supercell, with typical mesocyclone structure. The mesocyclone tightened and tornadogenesis occurred as S2′ (Fig. 1) grazed the back edge of the hook echo. The tornado, rated an F2 on the legacy Fujita scale was on the ground for 17 minutes (2145-2202 UTC) as it traveled its 11 km path. The storm eventually evolved into an HP supercell as it continued to produce hail and damaging winds downstream. It was even involved with yet another storm merger and subsequent weak tornado (see below), but as it moved into a far more stable environment east of the Atlanta Metro area, the storm eventually dissipated.

Supercell S8, unlike S1, developed approximately 25 km ahead of the dryline thus placing it in a region that had not been contaminated by surrounding convection. S8 showed characteristics of an LP supercell during the early part of its life. However, similar to S1 at the time of tornadogenesis, it too interacted with another cell, but this shower crossed the storm's inflow and was eventually ingested into the larger cell's WER. The tornado produced by this storm, rated an F3 on the legacy Fujita scale, was on the ground for six minutes as it traveled its 5 km path. Beginning as an LP supercell, the storm spanned the supercell spectrum during its long and cyclic life, briefly evolving into a classic and eventually into a long-lived HP supercell, from which additional tornadoes developed, all of which initiated by storm mergers or interactions.

This set of storms and the relationship relationships between them demonstrate how complex the nature of supercell storm evolution and tornadogenesis can become. Storm splits, mergers, and interactions took place within the unique evolution of at least two distinctly different supercell storm lifecycles. However, it seems clear from the data that in this event, each tornado occurred as a result of either a cell merger or at least non-merger interaction. While it may be difficult for warning forecasters to catch these interactions in real-time, it is crucial that meteorologists' situational awareness be heightened when these types of occurrences are possible.

Acknowledgements

Student participation for B. Miller was funded by the 2006 NOAA/Earnest F. Hollings Scholarship program. The authors would like to thank Dr. Christopher Weiss of Texas Tech University for his insights regarding dryline evolution and propagation. Thanks also to Dan Darbe, Michael Griesinger, and Gary Beeley (retired) in particular, as well as to several other meteorologists at WFO Peachtree City for their help and support throughout this study. In addition, we would like to acknowledge Jeff Evans, Rich Thompson, and David Imy from the SPC, Les Lemon from the NWS Warning Decision Training Branch, Kevin Pence from WFO Birmingham, AL, and Matt Bunkers from WFO Rapid City, SD, for their insights and expertise relevant to this event. Wendy Moen from WFO Charleston, SC, is also recognized for her assistance with respect to CAD erosion.

References

Bailey, C. M., G. Hartfield, G. M. Lackmann, K. Keeter, and S. Sharp, 2003: An objective climatology, classification scheme, and assessment of sensible weather impacts for Appalachian cold-air damming. *Wea. Forecasting*, 18, 641-661.

Bell G. D., and L. F. Bosart, 1988: Appalachian cold-air damming. *Mon. Wea. Rev.*, 116, 137–161.

Bluestein H. B., and C. R. Parks, 1983: A synoptic and photographic climatology of low-precipitation severe thunderstorms in the southern plains. *Mon. Wea. Rev*, 111, 2034–2046.

Bosart, L. F., 1975: New England coastal frontogenesis. *Quart. J. Roy. Meteor. Soc.,* 101**,** 957–978.

Businger S., W. H. Bauman III, and G. F. Watson, 1991: The development of the Piedmont front and

associated outbreak of severe weather on 13 March 1986. *Mon. Wea. Rev.*, 119, 2224–2251.
Craven J. P., H. E. Brooks, and J. A. Hart, 2002: Baseline climatology of sounding derived parameters associated with deep, moist convection. Preprints, *21st Conf. on Severe Local Storms,* San Antonio, TX, Amer. Meteor. Soc., 643–646.
Davies-Jones, R.P., D. Burgess, and M. Foster, 1990: Test of helicity as a tornado forecast parameter. Preprints, *16th Conf. on Severe Local Storms,* Kananaskis Park, AB, Canada, Amer. Meteor. Soc., 588–592.
Doswell, C. A., III, and D. W. Burgess, 1993: Tornadoes and tornadic storms: A review of conceptual models. *The Tornado: Its Structure, Dynamics, Prediction, and Hazards, Geophys. Monogr.,* 79, Amer. Geophys. Union, 161–172.
——, A. R. Moller, and R. W. Przybylinski, 1990: A unified set of conceptual models for variations on the supercell theme. Preprints, *16th Conf. on Severe Local Storms,* Kananaskis Park, AB, Canada, Amer. Meteor. Soc., 40–45.
Guyer, J. L., D. A. Imy, A. Kis, and K. Venable, 2006: Cool season significant (F2-F5) tornadoes in the Gulf Coast States. Preprints, *23d Conf. Severe Local Storms*, St. Louis MO., Amer. Meteor. Soc., CD-ROM, 4.2.
Hane, C. E., C. L. Ziegler, and H. B. Bluestein, 1993: Investigation of the dryline and convective storms initiated along the dryline: Field experiments during COPS-91. *Bull. Amer. Meteor. Soc.,* 74**,** 2133–2145.
Hane C. E., M. E. Baldwin, H. B. Bluestein, T. M. Crawford, and R. M. Rabin, 2001: A case study of severe storm development along a dryline within a synoptically active environment. Part I: Dryline motion and an Eta Model forecast. *Mon. Wea. Rev.*, 129, 2183–2204.
Johns, R. H., J. M. Davies, and P. W. Leftwich, 1993: Some wind and instability parameters associated with strong and violent tornadoes. Part II: Variations in the combinations of wind and instability parameters. *The Tornado: Its Structure, Dynamics, Prediction, and Hazards*. *Geophys. Mongr*., 79, Amer. Geophys. Union, 583-590.
Keeter K. K., S. Businger, L. G. Lee, and J. S. Waldstreicher, 1995: Winter weather forecasting throughout the eastern United States. Part III: The effects of topography and the variability of winter weather in the Carolinas and Virginia. *Wea. Forecasting*, 10, 42–60.
Lackmann, G. M., and W. M. Stanton, 2004: Cold-air damming erosion: Physical mechanisms, synoptic settings, and model representation. Preprints, *20th Conf. on Weather Analysis and Forecasting*, Seattle, WA, Amer. Meteor. Soc., CD-ROM, 8.3.
Lee, B. D., B. F. Jewett, and R. B. Wilhelmson, 2006: The 19 April 1996 Illinois tornado outbreak. Part II: Cell mergers and associated tornado incidence. *Wea. Forecasting*, 21, 449-464.
Markowski P. M., 2002: Hook echoes and rear-flank downdrafts: A review. *Mon. Wea. Rev.*, 130, 852–876.
——, J. M. Straka, and E. N. Rasmussen, 2002: Direct surface thermodynamic observations within the rear-flank downdrafts of nontornadic and tornadic supercells. *Mon. Wea. Rev*., 130, 1692-1721.
Moller A. R., C. A. Doswell III, M. P. Foster, and G. R. Woodall, 1994: The operational recognition of supercell thunderstorm environments and storm structures. *Wea. Forecasting*, 9, 327–347.
Palmer, T. D., B. A. Miller, L. P. Rothfusz, S. E. Nelson, submitted 2008: Analysis of cross-spectrum supercells during the north Georgia tornado event of 2 January 2006. *Natl. Wea. Digest.*
Rasmussen E. N., and D. O. Blanchard, 1998: A baseline climatology of sounding-derived supercell and tornado forecast parameters. *Wea. Forecasting*, 13, 1148–1164.
Rhea, J. O., 1966: A study of thunderstorm formation along drylines. *J. Appl. Meteor.,* 5**,** 58–63.
Richwein B. A., 1980: The damming effect of the southern Appalachians. *Natl. Wea. Dig.*, 5(1), 2–12.
Stanton, W. M., 2003: An analysis of the physical processes and model representation of cold air damming erosion. M.S. Thesis, Dept. of Marine, Earth, and Atmospheric Sciences, North Carolina State University, 224 pp.
Vescio, M. D., K. K. Keeter, G. Dial, P. Badgett, and A. J. Riordan, 1993: A low-top reflectivity severe weather episode along a thermal/moisture boundary in eastern North Carolina. Preprints, *17th Conf. on Severe Local Storms,* St. Louis, MO, Amer. Meteor. Soc., 628–632.
Wurman, J. M., Y. P. Richardson, C. Alexander, S. Weygant, P. F. Zhang, 2007: Dual-Doppler and single-Doppler analysis of a tornadic storm undergoing mergers and repeated tornadogenesis. *Mon. Wea. Rev*., 135, 736-758.